Medical Engineering & Physics 36 (2014) 196–204

Contents lists available at ScienceDirect

Medical Engineering & Physics

journal homepage: www.elsevier.com/locate/medengphy

Editor's comment: Thrombosis is a major complication of surgery, often with life-threatening consequences, and the failure to manage effectively blood coagulation and haemostasis is implicated in the failure of cardiovascular devices. While its relationship to blood flow, surface chemistry and haematological factors is well known, models that describe the kinetics of thrombus formation in patient-specific terms, and which are amenable to incorporation into large-scale numerical simulations, are few in number. The paper by Papadopoulos et al. presents a new phenomenological approach that draws on empirical data generated by thrombin generation assays to specify the parameters of interest. The model lends itself to the study of thrombus formation under realistic flow conditions according to the haematological status of the individual or patient.

Richard Black, Editor in Chief

A simplified mathematical model for thrombin generation

Konstantinos P. Papadopoulos*, Manolis Gavaises, Chris Atkin

School of Engineering and Mathematical Sciences, City University London, Room: C171, Northampton Square, London, EC1V 0HB, United Kingdom

ARTICLE INFO

Article history:
Received 28 May 2013
Received in revised form
30 September 2013
Accepted 15 October 2013

Keywords:
CFD
Coagulation
Simulation
Thrombus

ABSTRACT

A new phenomenological mathematical model based directly on laboratory data for thrombin generation and having a patient-specific character is described. A set of the solved equations for cell-based models of blood coagulation that can reproduce the temporal evolution of thrombin generation is proposed; such equations are appropriate for use in computational fluid dynamic (CFD) simulations. The initial values for the reaction rates are either taken from already existing model or experimental data, or they can obtained from simple reasoning under certain assumptions; it is shown that coefficients can be adjusted in order to fit a range of different thrombin generation curves as derived from thrombin generation assays. The behaviour of the model for different platelet concentration seems to be in good agreement with reported experimental data. It is shown that the reduced set of equations used represents to a good approximation a low-order model of the detailed mechanism and thus it can represent a cost-effective and-case specific mathematical model of coagulation reactions up to thrombin generation.

1. Introduction

The formation of thrombus in blood is involved in a number of life threatening situations like coronary artery disease and mechanical heart valve complications; it is a multi-scale phenomenon both in respect of time and space, involving a number of biochemical substances, blood circulating minerals and cellular responses. While the formation of blood clot is a physiological response of human body to vessel injury, it can be initiated when blood contacts certain substances like those exposed after the rupture of atheromatous plaques in stenosed vessels [1] and when pathological flow conditions prevail in a region [2]. Between the initiation and the formation of a thrombus, a series of enzymatic reactions takes place also known as coagulation cascade [3], classically divided in three parts: (1) the extrinsic or tissue factor (TF) pathway, (2) the intrinsic or contact pathway and the (3) common pathway. In every step of the process a circulating zymogen is activated, with the activation reaction being catalyzed by the products of previous steps. However, as most of these enzymatic reactions take place on cell membranes, the current approaches for coagulation are cell-based models and the process is divided in three discrete phases, initiation, amplification and propagation. Thrombin (factor IIa) and platelets play critical roles in the coagulation process. Thrombin in the final step catalyses the conversion of fibrinogen (factor I) to fibrin (factor Ia), a protein that through polymerization creates a mesh clot that also traps circulating blood cells. In addition, thrombin activates factor XIII (that forms bonds that crosslink the fibrin strands [4] causes the activation of platelets [5], the activation of factors V and VIII and their inhibitor protein C (APC). Platelets on the other hand, after activation by chemical or mechanical stimulation [6] become adhesive and form aggregates on the materials exposed after arterial damage [7] or plaque rapture [8,9] or in flowing blood. In addition they play a major role in thrombin formation [10,11] and they enhance the coagulation process by supporting on their membrane some of the coagulation reactions [12], releasing chemical substances and micro-particles [13] that influence the progress of coagulation and activate other platelets.

* Corresponding author. Tel.: +44(0)2070408115; fax:+44(0)2070408566.
E-mail addresses: Konstantinos.Papadopoulos.1@city.ac.uk (K.P. Papadopoulos), m.gavaises@city.ac.uk (M. Gavaises).

1350-4533/$ – see front matter © 2013 IPEM. Published by Elsevier Ltd. All rights reserved.
http://dx.doi.org/10.1016/j.medengphy.2013.10.012

The advance of computational techniques and increase of computational power have made possible the emergence of in silico studies that reproduce a part of or the whole process in greater or lesser detail, simulating either the whole process of thrombus formation or only the coagulation reaction system up to thrombin or fibrin production. The first mathematical simulation of thrombin and fibrin generation in plasma used exponential time functions as fixed inputs for concentration of some enzymes [14]. In vitro measurements of the reaction rate constants [15] were used for the development of a system of 20 reactions, including formation and breakage of complexes, in a study that mainly focused on the effect of variation of the concentration of different factors [16]. A similar model was proposed for the intrinsic pathway including fibrin production and APC inhibition mechanism, and was used to investigate threshold values for some enzymes and the spatial propagation of coagulation from the reacting site due to diffusion [17,18]. Subsequent work included more chemical substances and biochemical processes [19] up to thrombin production, resulting in a system consisting of 27 reactions and 42 reaction rate constants that later was combined with a Monte Carlo simulation method, in order to detect changes to the cascade initiation behaviour, due to small variation of the concentration of enzymes induced by the stochastic approach [20]. At the same time some studies used simulations to investigate a specific part of the coagulation cascade, as the function of positive feedback loops and threshold concentrations for cascade initiation [21], the triggering threshold with respect to tissue factor pathway inhibitor (TFPI) [22] or the inhibition mechanism of APC [23].

The studies that simulate thrombus formation and growth, simultaneously with blood flow and concentration of related substances, necessitate a less detailed sub-model for the coagulation cascade. While for the first studies of this kind the production rates of substances were mainly modelled as fluxes or with the use of few reactions [24,25], the increase of computational power allowed more complicated multi-scale and multi-phase models to emerge, that include an integrated coagulation sub-model. The authors in Kuharsky and Fogelson [26] proposed an integrated model of thrombus formation under flow conditions, taking into account the localization of reactions on surfaces, with the inclusion of the available binding sites on cell membranes for enzymes and using a system of 59 equations to simulate the coagulation system up to thrombin generation. A study that modelled platelet–platelet and platelet–wall interaction as reversible elastic links demonstrated the influence of these interactions on the flow field and predicted thrombus evolution and emboli formation [27]. The initial model was later improved with the addition of the APC mechanism and the transport of substances between plasma and endothelium cells [28]. The same concepts for cells and reactions were combined with an immersed boundary method [29,30] for modelling platelet movement and the interaction between platelet membrane sites and chemicals or endothelium. The results of this micro-scale model were also used to develop a continuous model for platelet aggregation (with platelets as continuous phase with movement limitations) describing the alterations in blood flow due to the presence of aggregated platelets [31] The macro-scale model was tested in simulations with pulsating flow in an idealized two dimensional vessel bifurcation [32]. The continuous model, with coupling of flow with thrombus growth and including flow and transport within the thrombus, was used to demonstrate the effects of flow conditions and the quantity of TF exposed in thrombus growth [33]. Anand et al. [34,35] presented another multi-process model that used a viscoelastic model to simulate flow for both free vessel lumen and clot. This model also incorporated the activation of platelets due to excessive shear stress and fibrin production and lysis. In a similar work, a model for the viscosity of blood depending on fibrin concentration was proposed and used in a three-dimensional simulation of blood coagulation in a tube with a reacting site; in this study the area where fibrin concentration exceeded a specific value interpreted as the area occupied by the clot [36]. In Xu et al. [37] another multi-scale model was proposed that included a cellular pot model [38] for discrete cells and cell movement was simulated through an energy-based stochastic process. The simulation involved differentiation of cell movements depending on fibrin levels and cell–cell or cell–surface interaction and bonds. The model was used to evaluate the role of fVII in venous thrombus formation due to vessel injury [39] and to examine the impact of pulsating flow and the non-Newtonian characteristics of blood on thrombus growth [40].

While the detailed description of coagulation included in these works makes them appropriate for studying the influence of different factors, unfortunately it increases dramatically the computational cost; thus published applications mainly refer to small two dimensional regions ($\sim$100 μm) while the dimensions of computational regions for studying thrombus formation in a coronary artery or in mechanical heart valves are much larger (typically, the diameter of the coronary artery is about 4 mm while the diameter of the aortic root is of some cm) with the flow distribution being three-dimensional and strongly time dependent preventing use of simplified flow models. In addition, these models do not have patient-specific characteristics, as the use of reaction rate constants derived from experiments do not allow the significant variability of thrombin generation observed for different individuals [41]. At the same time, it has been shown that the resulting thrombin generation curve predicted by such models under steady state conditions can be simulated in different ways by a much simpler system of 6 equations [42]. As the process between the initial stimulation and the formation of thrombin consist the main part of the coagulation reactions, our motivation is to develop a phenomenological model for thrombin formation that would be efficient enough to be used with three dimensional computational fluid dynamic (CFD) simulations while also being adjustable in order to reflect measured differences existing in data of different individuals. A case-specific simplified model like this, though not including the full biochemical details of the process, could be used for comparison of different cases of clinical interest.

2. Materials and methods

The aim of the study is to propose a set of equations that describe the thrombin generation in blood using the minimum possible number of parameters but which are able to describe with acceptable accuracy the whole process. The model is validated against experimental results for thrombin generation in vitro from Thrombin Generation Assays (TGA). The proposed model for thrombin production is based on the cell-based models of coagulation [12]; the full description of the biochemical processes are mainly based on Hoffman and Monroe [11]. For a detailed modelling of coagulation the localization of the different reactions makes the task more complicated, as it requires taking into account additional parameters such as the binding rate of the substances on cell membranes and the expression, concentration and availability of appropriate binding sites on the cell surfaces. For the development of a simplified model however, it can function as an advantage, as the processes can be grouped in respect to the location they occur (on platelet surface, on the vessel wall or in plasma). This approach is rigorous in cases where the transport of reactants is mainly due to convection such as arterial flow conditions, or in cases where the different species are well mixed. The generation of thrombin and generally the coagulation process is mainly attributed to activated platelets, while the initiation phase is localized on the reacting site of the vessel surface. The burst of thrombin generation is considered to occur when the small amounts of thrombin

Table 1
Equations of the model.

Thrombin (IIa)	$\frac{\partial[IIa]}{\partial t} = -k_{in}[IIa] + (k_{surf} + k_{II}^{AP} \cdot [AP]) \cdot [II]$
Prothrombin (II)	$\frac{\partial[IIa]}{\partial t} = -(k_{surf} + k_{II}^{AP} \cdot [AP]) \cdot [II]$
Activated platelets (AP)	$\frac{\partial[AP]}{\partial t} = k_{AP}^{AP} \cdot [AP] \cdot [RP] + k_{AP}^{IIa} \cdot [RP]$
Resting platelets (RP)	$\frac{\partial[RP]}{\partial t} = -k_{AP}^{AP} \cdot [AP] \cdot [RP] - k_{AP}^{IIa} \cdot [RP]$

produced during the initiation phase cause thrombin concentration to exceed a threshold value. The threshold values used are within the range of thrombin concentration values that have been reported in Rosing et al. [10] as being capable of causing platelet activation, 0.5–1.2 nM of thrombin (0.05–0.12 U/ml). The equations of the model are shown in Table 1. The initial values for the reaction rate constants, shown in Table 2, are taken either from already existing models or from experimental studies.

As the proposed model used a reduced number of 4 reactions, each reaction rate represents the integral effect of more than one actual process. Also, 'activated platelets' actually represent platelet activity, in the sense that 100% activated platelets implies maximum platelet activity rather than the fact that all platelets are activated. Fig. 1a illustrates the actual biochemical reactions that influence each constant while Fig. 1b the reduced model. The model is structured as follows: During the initiation phase thrombin generation is described by a slow first order reaction. This reaction, which is localized on the TF-bearing cells, is used to describe the whole pro-coagulant activity that occurs on the TF-bearing cells – formation of the TF–VIIa complex, activation of factors IX, X and V. In this reaction is also included the inhibition of the amounts of IXa, Xa that leave the cell surfaces by TFPI in plasma. The initial value for the reaction rate constant was estimated using the lag times reported in Lawson et al. [15]; van't Veer and Mann [43]. Inhibition of thrombin during this phase is also modelled as a first-order reaction, with the value of the reaction rate constant for thrombin inhibition calculated from the IIa ·ATIII inhibition reaction, using the initial bulk concentration of ATIII ($k_{in} = k_{in,ATIII} \cdot \varphi_{ATIII,0} = 1.71 \times 10^{-2}\ s^{-1}$), as this reaction is the major process of thrombin inhibition (thrombin inactivation is 77% by anti-thrombin, 14% a_2 macroglobulin and 9% by minor inhibitors [44]). With this setup for the initiation phase, the model describes the threshold behaviour of the initiation of blood coagulation in respect to TF concentration [45,46], as there is a minimum value of activation constant capable of causing thrombin burst and, as this constant is related to the TF concentration (see Section 4), a threshold value for TF concentration.

Beyond the point that thrombin concentration has reached the threshold value, the conversion of prothrombin to thrombin is mainly attributed to platelets after their activation. This process is modelled as a second-order reaction, with the initial values for the reaction rate constant used from Rosing et al. [10]; Sorensen et al. [47]. Platelets can be activated either by thrombin, if its concentration is greater than the threshold value, or directly by other activated platelets. Thrombin in concentration about 1 nM can initiate the activation of platelets [48], from 0.5 nM for minimum activity to 1.2 nM for maximal [10]. Platelet activation by thrombin is modelled as a first-order reaction that is initiated when thrombin concentration reaches the threshold value. The activation of platelets by activated platelets represents the activation by platelet-released substances and is modelled as a second order reaction. The reaction rate constants for the activation of platelets used were found in Kuharsky and Fogelson [26]. In the case of TF induced coagulation the contribution of the later reaction is negligible, but it can make the model capable of being used to describe shear induced coagulation.

Inhibition of thrombin during the propagation phase is again modelled as a first-order reaction. The reaction rate constant for the inhibition of thrombin in plasma is not the same as for the initiation phase; here we must note that this constant is significantly smaller than the one used in Leiderman and Fogelson [33] for modelling this reaction in the same manner, which was based on thrombin half-life in plasma. However, as the activation of protein C that acts as an inhibitor to the coagulation process mainly occurs on the endothelium cells, for the areas near the endothelium cells the value used for thrombin inhibition is larger, with the exact value derived from the adjustment of the model with the use of TGA results. As demonstrated in Fig. 2, the model using the initial parameter values gives reasonable results. By adjusting the values of the constants and parameters of the model within physiological limits, the model can reproduce, to a good level of accuracy, actual thrombin production, by considering the four main parameters of a thrombin generation assay: lag-time (T_{lag}), maximum concentration (C_{max}), time until thrombin concentration reaches the maximum (T_{max}) and the estimated thrombin potential (ETP); the last one is represented by the surface under the curve in a thrombin concentration vs time graph. The initial attempts of adjustments were performed manually, but in general the adjustment can be done using the following procedure and assumptions.

Platelet response is very fast compared to the other processes included in the model [49,50]. With the approximation that all platelets are activated as soon as thrombin concentration reaches the threshold value, the system of the equations can be analytically solved, giving the equation that describes thrombin concentration through time. This equation has the general form (see Appendix 1a):

$$[IIa](t) = \frac{B_i}{A_i - C_i}(e^{A_i t} - e^{C_i t}) = F(t)$$

The equation is similar to the equation proposed in Wagenvoord et al. [42] but in a non-uniform platelet distribution the results will vary in space. Here the constants A, B and C depend both on the model parameters and TAG results, and they have different values for the initial phase and the propagation phase.

Using the parameters of the TGA and this function we obtain the equations

$$F(T_{lag}) = [IIa]_{thr}$$

$$F(T_{max}) = C_{max}$$

Table 2
Constants and parameters.

Process	Constant symbol	Initial value (S.I.))	Reference
Thrombin generation by activated platelets	k_{II}^{AP}	0.856–1.81 s^{-1}	[10,47]
Thrombin generation on reacting surface	k_{surf}	$10^{-5}\ s^{-1}$	n/a
Platelet activation by thrombin	k_{AP}^{IIa}	0, *if* $[IIa] < [IIa]_{thr}$ 0.5, *if* $[IIa] \geq [IIa]_{thr}$	[26,47]
Platelet activation by activated platelets	k_{AP}^{AP}	$5.24 \times 10^{-2}\ s^{-1}$	[26]
Thrombin inhibition*	k_{in}	1.71×10^{-2}–$0.2\ s^{-1}$	[19,33]
Thrombin concentration threshold for platelet activation	$[IIa]_{thr}$	$1.75–4.18 \times 10^{-8}$ kg/kg (0.5–1.2 nM or 0.05–0.12 U/ml)	[10]

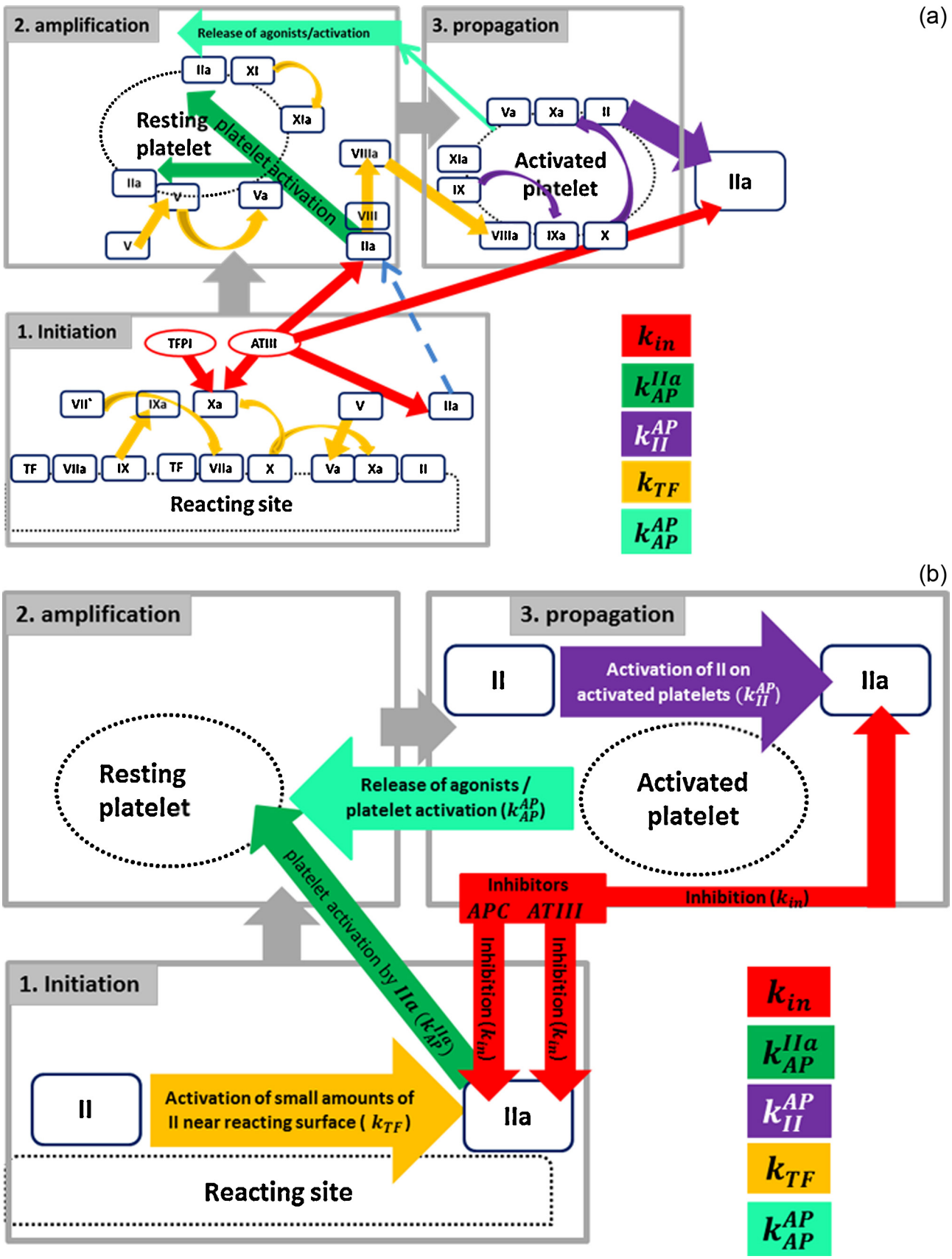

Fig. 1. Schematic representation of cell based model for blood coagulation (reproduced from Smith et al. [12]). (a) and the reduced model (b). The different coloured arrows represent the actual processes that are lumped in each reaction rate constant. Red: Inhibition of thrombin in plasma by ATIII and near the vessel wall by APC. Green: Platelet activation by thrombin. Purple: thrombin production by activated platelets. Yellow: Thrombin production in plasma near the reacting site on vessel wall, includes all the reactions from binding of VIIa on TF up to the generation of small amounts of IIa and also (mostly) the inhibition of all other species except thrombin. Turquase: Activation of platelets by substances released by activated platelets such as ADP. (For interpretation of the references to colour in this figure legend, the reader is referred to the web version of the article.)

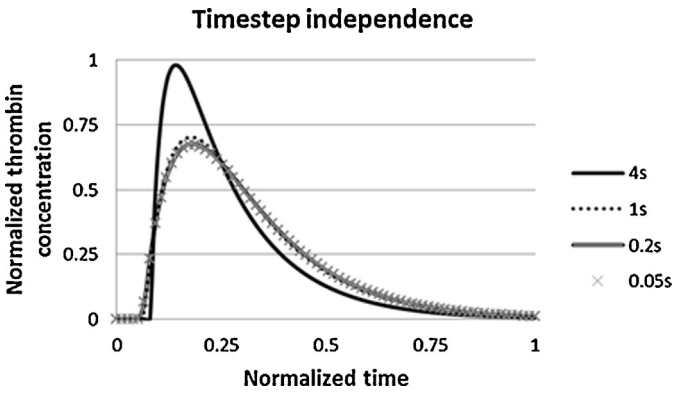

Fig. 2. Results of the model for different time steps. For time steps below 0.5 s the results coincide.

$$\frac{dF}{dt}(T_{\max}) = 0$$

$$\int_0^{\infty} F(t)dt \cong \int_{T_{lag}}^{t\infty} F(t)dt = ETP$$

From this set of equations the constants of the model can be approximated numerically, making the resulting model equations able to reproduce with the curve of a TGA with given parameters. In most of the following results only the constants related to thrombin production k_{II}^{AP}, k_{surf}, k_{in} (see Table 1) were adjusted. In case data from the whole curve is available, the constants can be approximated as described in Appendix 1b.

3. Results

We first applied the model using the initial values for the constants; while the resulting curve has the shape of a typical thrombin generation curve, the actual values were significantly higher than the typical results of TGA for fresh platelet rich plasma as reported in Gerotziafas et al. [51]. Performing simulations for different time steps, we found that the results of the model are identical for time steps below 0.5 s (Fig. 2). As a whole heart cycle at rest conditions is about 0.8 s (for 75 bpm), the maximum magnitude of the time steps for simulating pulsating flow is much smaller, thus in terms of temporal discretization, the coupling of the model with CFD simulations can be straightforward.

Subsequently we applied the model in 8 different cases, denoted as Cases 1–8. In the plots, when both model and experimental results are represented, model results are named 'C# model' and the experimental results 'C# exp'. The equations for the adjustment of the constants were solved in MATLAB, while the adjustment of the platelet related constants was done manually using Excel and Systems Biology Toolbox 2 [52]. Case 1 represents the tuning of the model constants in order to reproduce typical TGA results as reported in Gerotziafas, Depasse et al. [51] and the resulting curve (C1 model) is shown in Figs. 3 and 4, compared with curves representing slower thrombin generation. In the absence of inhibition (cases 2 and 3), the time interval between the end of the initiation phase and the moment that thrombin concentration reaches its maximum value is 2–4 min, depending on the constant for thrombin activation by activated platelets, and the results match approximately the experimental thrombin production curves found in Lawson et al. [15] (Fig. 5).

The next test (Case 4) involved adjusting the model constants in order to fit an arbitrary thrombin generation curve. The experimental curve was found in Hemker et al. [53]. Fig. 6 shows that

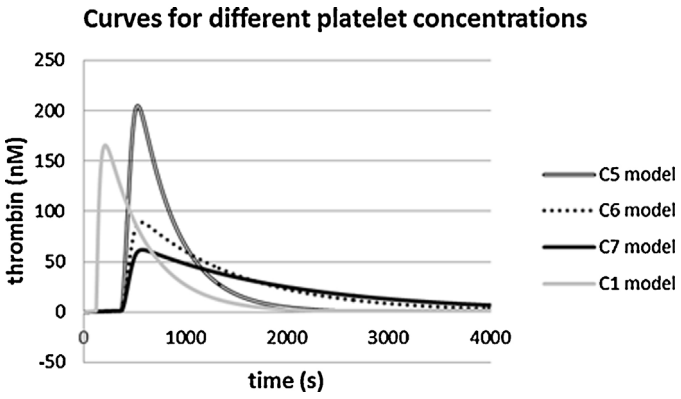

Fig. 3. Behaviour of the model for different initial platelet concentrations.

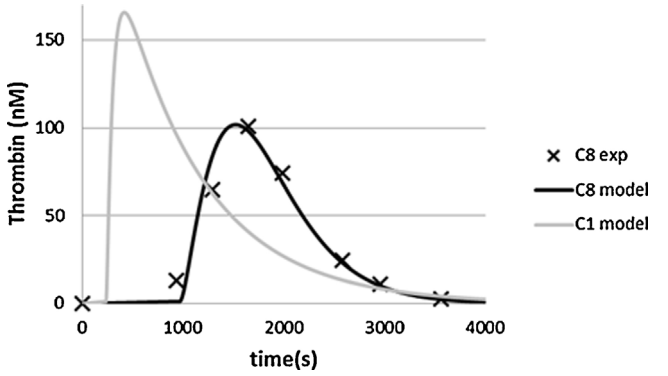

Fig. 4. Adjustment of the model in order to reproduce slower thrombin generation, experimental data.

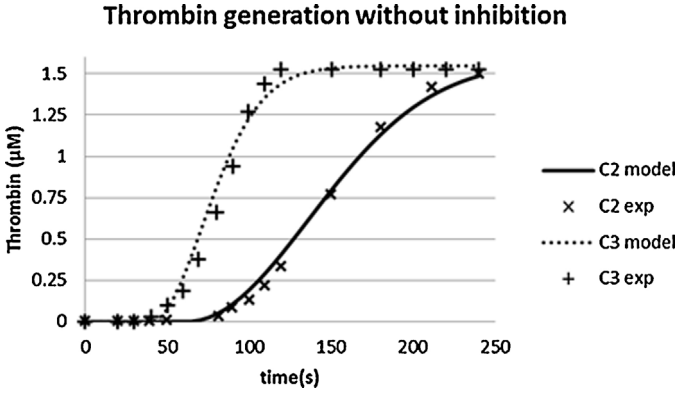

Fig. 5. Model results for thrombin production without inhibition, adjusted to fit the results reported in Lawson et al. [15].

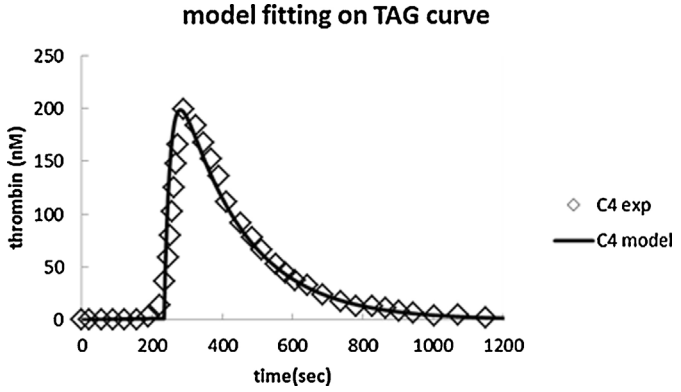

Fig. 6. Capability of the model to reproduce an arbitrary thrombin generation curve [62].

Table 3
Results of the model for different cases.

		T_{lag} (min)	T_{max} (min)	C_{max} (nM)	ETP (nM min)
Case 1	Experiment	3.6 ± 0.8	7.4 ± 1.8	164 ± 50	1321 ± 330
	model	3.7	6.8	165	1364
Case 2	Experiment	1.5	3.5	(1.5×10^3)	n/a
	model	1.5	4	(1.5×10^3)	n/a
Case 3	Experiment	0.67	2.25	(1.5×10^3)	n/a
	model	0.65	2.38	(1.5×10^3)	n/a
Case 4	Experiment	3.5	4.8	199	735
	model	3.7	4.6	196	710
Case 5	Experiment	5 ± 0.5	11 ± 2.7	161 ± 38	1633 ± 81
	model	5.8	9	190	1718
Case 6	Experiment	5.5 ± 0.5	11 ± 0.2	98 ± 40	1316 ± 255
	model	6	9.4	91	1370
Case 7	Experiment	5.8 ± 0.7	13 ± 0.9	72 ± 38	1135 ± 300
	model	6	9.6	62	1118
Case 8	Experiment	15	27	101	2012
	model	13.3	25.3	102	1934

the model predicts the experimental curve with good accuracy. For future application of the model under flow conditions characterized by non-uniform concentrations of platelets, it has been considered important to test its behaviour with given constants for varying concentration of platelets near to the physiological values. We adjusted the constants so that the model approximated the TGA results for platelet concentration 150×10^9 pl/L (physiological values are 200–400 $\times 10^9$ pl/L) and then applied the model with the same setup for two other values of platelet concentrations; Cases 5–7 use the same values for reaction rate constants with platelet concentration 400, 150 and 100 $\times 10^9$ pl/L respectively. The results shown in Table 3 are within the range of values reported in Gerotziafas et al. [51] although the dependence of maximum concentration of thrombin on platelet concentration seems a little stronger than for the in vitro experiments. The resulting curves are shown in Fig. 3. Further increase of platelet concentration resulted in higher values for maximum thrombin concentration and small decrease of T_{max}, without significant effect on ETP. If the constants describing platelet activation are also suitably modified, the equations can match curves that depict slower thrombin formation like the ones reported in [54] for lower platelet concentrations (75×10^9 pl/L) as shown in Fig. 4. The values of the model constants after modification, in order to fit different cases, are shown in Table 4 and for all cases the values are within a reasonable range.

4. Discussion

This work presents a phenomenological model for thrombin generation that is flexible enough to reproduce a wide range of cases and simple enough to be used for modelling thrombin generation in large scale CFD simulations – in contrast with the most recently suggested models. The four equations of the model are based on the principle assumption that all reactions occur either on the platelet surface or on the reacting site of the vessel wall.

The reactions related to platelet activation actually represent the transition from the initiation to the propagation phase. As the curves used to reproduce a wide range of TGA results correspond to different experiments, these constants vary significantly between two groups of Cases. In the experiments for Cases 1–4, where phospholipids have been used as a substrate for enzymatic reactions, this transition is much faster than for Cases 5–8 where human platelets have been used. For Cases 5–8 the values of these constants have been adjusted manually. It is interesting that the calculated time until platelets reach half of the maximum activity for Case 8 is 5–10 min, in agreement with Allen et al. [54]. However, as reported recently from Ninivaggi et al. [55], TGA results in whole blood resemble the curves of Cases 1 and 4 (possibly because red blood cells that are not included in most TGA also contribute to thrombin generation [55,56]) so this modification of the parameters related to platelet activation is not necessary for physiological cases and the model can be calibrated as described above. On the other hand with the use of such modifications the model could also approximate pathological cases as haemophilia or thrombin generation after anticoagulation treatment. In contrast to the methods described and reviewed in Brummel-Ziedins [57] where the effect of the variation of each factor concentration and activity is investigated, this model uses only the information included in the TGA curve, thus it has some limitations. For a given value of inhibition reaction rate, has a maximum lag time that it can reproduce if the reported lag time is greater than this maximum value, modification of the inhibition constant is required. Curves corresponding to pathological situations as severe haemophilia A [42] can be approximated. As factor VIII is mainly involved in the propagation phase, it is expected that in order to reproduce curves for different fVIII concentrations the related constants (k_{in}, k_{AP}^{IIa} and k_{IIa}^{AP}) (should be modified. As shown in Fig. 8, this can be done (the concentrations of VIII have been calculated using 12.8 hours as half-life of fVIII [58]). At first sight, the most significant inaccuracy of the model (when the initial values of the parameters are used) is that the time interval between the initiation of thrombin burst and maximum concentration of thrombin is smaller than the one reported in TGAs (2.8 min compared to 2 min predicted by the model) when adjusting only the three previously mentioned parameters. The increase of thrombin concentration predicted by the model is sharper compared to the experimental data and the shapes of the two curves differ for this time interval. That can be fixed by adjusting manually the constants related to platelet activation as we did for Cases

Table 4
The variation of the model constants after adjustment in order to reproduce different cases.

Constant	Initial estimations	Case 1	Case 2	Case 3	Case 4	Cases 5–7	Case 8
k_{surf} (s^{-1})	10^{-5}	7.367×10^{-6}	9.162×10^{-6}	1.511×10^{-5}	7.367×10^{-6}	7.223×10^{-6}	4.06×10^{-7}
k_{II}^{AP}(s^{-1})	0.0856–1.81	0.73	2.8	4	1.55	0.525	3.6
k_{in}(s^{-1})	1.71×10^{-2}–0.2 s^{-1}	0.032	0	0	0.052	0.0262	0.024
k_{AP}^{IIa}(s^{-1})	0.2–0.5	–	–	0.5	0.5	0.002	0.0018

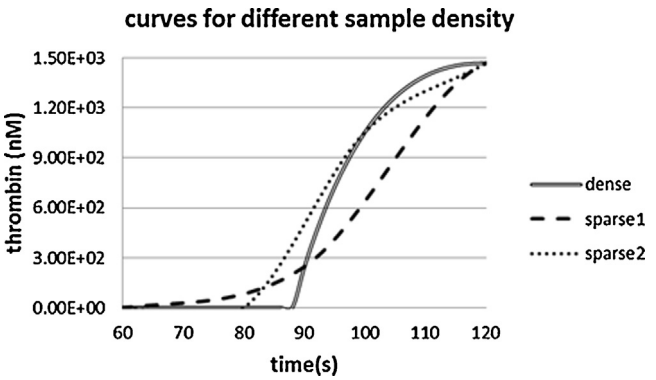

Fig. 7. Dependence of the shape of the curve on the time interval between two data points. While the initial results are the same curve fitting on data produces significantly different curves.

4–8. However the experimental data, while in all studies presented in the form of curves, in some cases actually correspond to measurements in discrete time intervals and the resulting curves are obtained through data fitting. In Fig. 7 a plot of three curves is shown, for the time interval of thrombin concentration increase, obtained from the same model results. In one case (dense) the time interval between two data points is 2 s, while for the other two cases (sparse1 and sparse2) is 30 s and 20 s respectively –reasonable time intervals between the withdrawal of two samples. It is obvious that curve fitting on experimental values, used in studies prior to the introduction of continuous monitoring of thrombin generation, while making the results more presentable can also give incorrect information on the actual evolution of the process between two measurements, so differences between modelled and experimental curves do not necessary indicate inadequacy of the model.

The constant that represents the initial thrombin production rate k_{surf} (for a given value of the inhibition rate) is mainly determined by the lag time. While there is dependence of different experiments' results on the exact composition of the samples and the triggering substance used, for the case described in; Gerotziafas et al. [51], there seems to be a clear relationship ($R^2 = 0.989$) between TF concentration and k_{surf} for the same experimental conditions and TF concentrations between 1 and 30 pM:

$$k_{surf} = k_{surf,\max}\left(A + B\ln\left(\frac{[TF]}{[TF_{\max}]}\right)\right)$$

The constant values are $A = 0.996 \approx 1$, $B = 0.0372$ while for the aforementioned study the maximum calculated value for the rate of thrombin generation during the initiation phase is $k_{surf,\max} = 7.91 \times 10^{-6}\,s^{-1}$ and the relationship can approximately be written as:

$$k_{surf} = k_{surf,\max}\left(1 + 0.0372 \cdot \ln\left(\frac{[TF]}{[TF_{\max}]}\right)\right)$$

These relationship gives good result when estimating k_{surf} in other studies with similar methodology, but for studies using recombinant TF:VIIa [15,43] as trigger for the coagulation process, while the a good correlation between k_{surf} and trigger concentration can be established, ($R^2 > 0.98$) the resulting formulas are different.

For the case of thrombus formation on a reacting site of a blood vessel wall, the term representing the slow phase of thrombin generation corresponds to a surface reaction term. The reaction rate for the surface reaction can be calculated with the use of the reported surface TF concentration in atheromatous plaques (33 pg/cm^2) [59] and the molecular weight of (46,000 Da approximately [60]). For a computational cubic cell of e.g. 100 μm this numbers would lead to a TF concentration of about 70 pM resulting to $k_{surf} = 9.75 \times 10^{-6}\,s^{-1}$. Sub-threshold concentration of thrombin actually represents also the products of the previous steps of coagulation. At the same time this approach allows a slow rate of fibrin production before the burst of thrombin and a realistic prediction of clotting time. As TGA results demonstrate inter-laboratory variation [61] this model, based on TGA results and with its simplified character, does not claim to reproduce with precise accuracy thrombin generation but offers a way to model thrombin generation that (1) has comparative value, in the sense that it can be adjusted to describe different rates of thrombin generation, and (2) can be easily coupled with CFD simulations. We believe that these

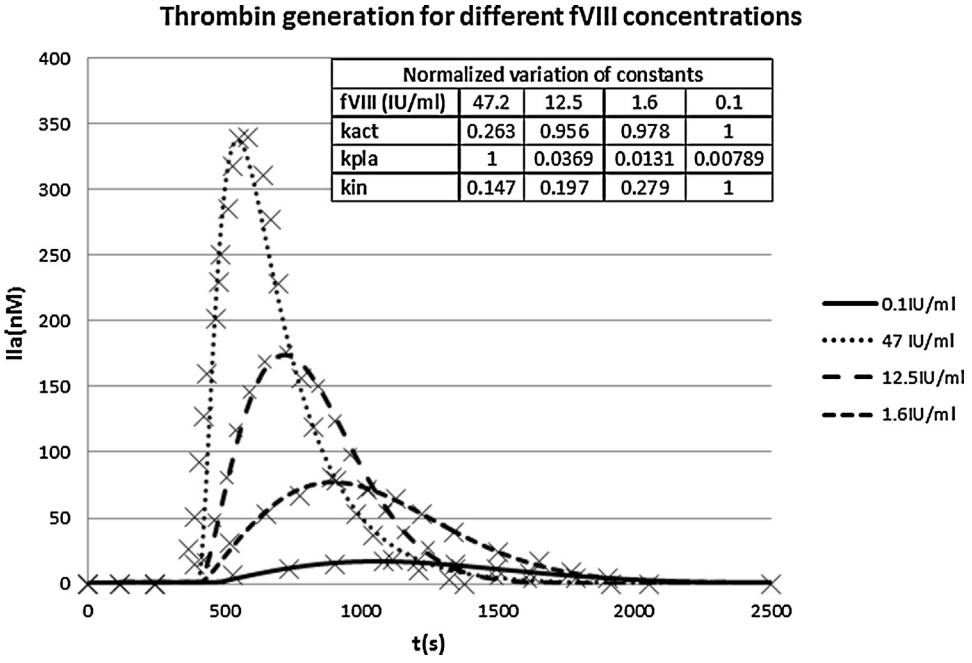

Fig. 8. Reproduction of thrombin generation curves corresponding to different fVIII concentrations and the normalized modification of the related constants.

equations, if combined with two more, one describing fibrin formation and one describing platelet deposition on the reacting site of the vessel, can be used as a thrombus formation model for three dimensional CFD simulations in blood vessels. The results of such a model can be used to compare the evolution of thrombus formation in different cases and for different thrombogenic potential of human blood. Finally, as the model describes the production of thrombin in blood in a phenomenological way, it does not require additional information regarding the concentration of different factors and the details for every reaction in the coagulation system and it can be calibrated and applied directly for different cases based only on the parameters or the curve of the TGA (or the curve itself).

Funding

None.

Ethical approval

Not required.

Appendix. Equations' solution

a. Under the assumption that all platelets are instantly activated when thrombin reaches its threshold value, the concentration of platelets is zero when thrombin concentration is below the threshold value and equal to the resting platelet concentration when thrombin exceeds the threshold values. The equations describing thrombin and prothrombin concentration become:

$$\frac{\partial[IIa]}{\partial t} = -k_{in}[IIa] + k_{tot} \cdot [II]$$

$$\frac{\partial[II]}{\partial t} = -k_{tot} \cdot [II]$$

Here k_{tot} represent the total rate of prothrombin conversion to thrombin and includes both the production on the reacting site and on the platelet surfaces:

$$k_{tot} = k_{surf} + k_{II}^{AP} \cdot [PL], \quad if\ [IIa] > [IIa]_{th}$$
$$k_{tot} = k_{surf}, \quad if\ [IIa] \le [IIa]_{th}$$

This leads to a direct solution for prothrombin concentration:

$$[II](t) = [II](t=0) \cdot e^{-k_{tot} \cdot t}$$

The D.E. describing thrombin concentration becomes:

$$\frac{\partial[IaI]}{\partial t} = -k_{in}[IIa] + k_{tot} \cdot [II_o] \cdot e^{-k_{tot} \cdot t}, \text{ or } \frac{dx}{dt} = Ax - CBe^{Ct}$$

where $A = -k_{in}$, $B = [II]_o$ and $C = -k_{tot}$

The equation can be rewritten as follows:

$$\frac{dy}{dt} = (A - C) \cdot y - CB, \text{ where } y = x \cdot e^{-Ct}$$

The last expression, after manipulation leads to an (approximate because of the aforementioned assumption) analytic solution for the temporal evolution of thrombin concentration (X):

$$X(t) = \frac{e^{Ct}}{A - C} = [((A - C)X_0 e^{-Ct_0} - CB)e^{(A-C)t} + CB)] \text{ or}$$

$$[IIa](t) = \frac{e^{-k_{tot} \cdot t}}{k_{tot} - k_{in}}[((k_{tot} - k_{in})[IIa]_0 e^{k_{tot} \cdot t_0} + k_{tot} \cdot [II]_o)e^{(k_{tot} - k_{in}) \cdot t} - k_{tot} \cdot [II]_o]$$

For $[IIa](t=0) = 0$ the equation gets the simplified form:

$$[IIa](t) = \frac{k_{tot} \cdot t[II]_o}{k_{in} - k_{tot}}(e^{-k_{tot}t} - e^{-k_{in} \cdot t})$$

b. In the case the data from the whole curve is available, there is another way for obtaining the model constants. The reaction rate is obtained by solving (numerically) the last equation:

$$[IIa]_{th} - \frac{k_{surf} \cdot [II]_o}{k_{in} - k_{tot}}(e^{-k_{surf}T_{lag}} - e^{-k_{in} \cdot T_{lag}}) = 0$$

As the activated platelet concentration is approximately,

$$[AP] = [RP](0)(1 - e^{-(t - T_{lag})k_{AP}^{IIa}}),\ t > T_{lag}$$

Analytical expression can be obtained for prothrombin concentration versus time, $[II](t) = [II](t=0) \cdot e^{-k_{tot}(t) \cdot t}$ and therefore for the differential equation describing thrombin evolution for $t > T_{lag}$, $d/dt[IIa] = -k'_{in} \cdot [IIa] + k_{tot}(t) \cdot [II](t)$ and the constants can be obtained numerically using an iterative process.

Conflict of interest statement

None declared.

References

[1] Rauch U, Osende JI, Fuster V, Badimon JJ, Fayad Z, Chesebro JH. Thrombus formation on atherosclerotic plaques: pathogenesis and clinical consequences. Ann Intern Med 2001;134:224–38.
[2] Nesbitt WS, Westein E, Tovar-Lopez FJ, Tolouei E, Mitchell A, Fu J, et al. A shear gradient-dependent platelet aggregation mechanism drives thrombus formation. Nat Med 2009;15:665–73.
[3] Furie B, Furie BC. Mechanisms of thrombus formation. N Engl J Med 2008;359:938–49.
[4] Mosesson MW. Fibrinogen and fibrin structure and functions. J Thromb Haemost 2005;3:1894–904.
[5] Brass LF. Thrombin and platelet activation. Chest J 2003;124:18S–25S.
[6] Jesty J, Yin W, Perrotta P, Bluestein D. Platelet activation in a circulating flow loop: combined effects of shear stress and exposure time. Platelets 2003;14:143–9.
[7] Badimon L, Badimon JJ, Galvez A, Chesebro JH, Fuster V. Influence of arterial damage and wall shear rate on platelet deposition. Ex vivo study in a swine model. Arterioscler Thromb Vasc Biol 1986;6:312–20.
[8] Fernández-Ortiz A, Badimon JJ, Falk E, Fuster V, Meyer B, Mailhac A, et al. Characterization of the relative thrombogenicity of atherosclerotic plaque components: implications for consequences of plaque rupture. J Am Coll Cardiol 1994;23:1562–9.
[9] Reininger AJ, Bernlochner I, Penz SM, Ravanat C, Smethurst P, Farndale RW, et al. A 2-step mechanism of arterial thrombus formation induced by human atherosclerotic plaques. J Am Coll Cardiol 2010;55:1147–58.
[10] Rosing J, van Rijn J, Bevers E, van Dieijen G, Comfurius P, Zwaal R. The role of activated human platelets in prothrombin and factor X activation. Blood 1985;65:319–32.
[11] Monroe DM, Hoffman M, Roberts HR. Platelets and thrombin generation. Arterioscler Thromb Vasc Biol 2002;22:1381–9.
[12] Smith SA. The cell-based model of coagulation. J Vet Emerg Crit Care 2009;19:3–10.
[13] Rendu F, Brohard-Bohn B. The platelet release reaction: granules' constituents, secretion and functions. Platelets 2001;12:261–73.
[14] Willems G, Lindhout T, Hermens WT, Hemker H. Simulation model for thrombin generation in plasma. Pathophysiol Haemost Thromb 1991;21:197–207.
[15] Lawson JH, Kalafatis M, Stram S, Mann KG. A model for the tissue factor pathway to thrombin. I. An empirical study. J Biol Chem 1994;269:23357–66.

[16] Jones KC, Mann KG. A model for the tissue factor pathway to thrombin. II. A mathematical simulation. J Biol Chem 1994;269:23367–73.
[17] Zarnitsina VI, Pokhilko AV, Ataullakhanov FI. A mathematical model for the spatio-temporal dynamics of intrinsic pathway of blood coagulation. II. Results. Thromb Res 1996;84:333–44.
[18] Zarnitsina VI, Pokhilko AV, Ataullakhanov FI. A mathematical model for the spatio-temporal dynamics of intrinsic pathway of blood coagulation. I. The model description. Thromb Res 1996;84:225–36.
[19] Hockin MF, Jones KC, Everse SJ, Mann KG. A model for the stoichiometric regulation of blood coagulation. J Biol Chem 2002;277:18322–33.
[20] Lo K, Denney WS, Diamond SL. Stochastic modeling of blood coagulation initiation. Pathophysiol Haemost Thromb 2005;34:80–90.
[21] Beltrami E, Jesty J. Mathematical analysis of activation thresholds in enzyme-catalyzed positive feedbacks: application to the feedbacks of blood coagulation. Proc Natl Acad Sci USA 1995;92:8744–8.
[22] Xu C, Hu Xu X, Zeng Y, Wen Chen Y. Simulation of a mathematical model of the role of the TFPI in the extrinsic pathway of coagulation. Comput Biol Med 2005;35:435–45.
[23] Qiao YH, Xu CQ, Zeng YJ, Xu XH, Zhao H, Xu H. The kinetic model and simulation of blood coagulation – the kinetic influence of activated protein C. Med Eng Phys 2004;26:341–7.
[24] Hubbell JA, McIntire LV. Platelet active concentration profiles near growing thrombi. A mathematical consideration. Biophys J 1986;50:937–45.
[25] Folie BJ, McIntire LV. Mathematical analysis of mural thrombogenesis. Concentration profiles of platelet-activating agents and effects of viscous shear flow. Biophys J 1989;56:1121–41.
[26] Kuharsky AL, Fogelson AL. Surface-mediated control of blood coagulation: the role of binding site densities and platelet deposition. Biophys J 2001;80:1050–74.
[27] Fogelson AL, Guy RD. Platelet–wall interactions in continuum models of platelet thrombosis: formulation and numerical solution. Math Med Biol 2004;21:293–334.
[28] Fogelson AL, Tania N. Coagulation under flow: the influence of flow-mediated transport on the initiation and inhibition of coagulation. Pathophysiol Haemost Thromb 2005;34:91–108.
[29] Lai M-C, Peskin CS. An immersed boundary method with formal second-order accuracy and reduced numerical viscosity. J Comput Phys 2000;160:705–19.
[30] Peskin CS. The immersed boundary method. Acta Numerica 2002;11:479–517.
[31] Fogelson AL, Guy RD. Immersed-boundary-type models of intravascular platelet aggregation. Comput Meth Appl Mech Eng 2008;197:2087–104.
[32] Yang XS, Lewis RW, Zhang HY. Finite element analysis of fogelson's model for platelet aggregation. In: European Congress on Computational Methods in Applied Sciences and Engineering (ECCOMAS 2004). 2004.
[33] Leiderman K, Fogelson AL. Grow with the flow: a spatial–temporal model of platelet deposition and blood coagulation under flow. Math Med Biol 2011;28:47–84.
[34] Anand M, Rajagopal K, Rajagopal KR. A model incorporating some of the mechanical and biochemical factors underlying clot formation and dissolution in flowing blood. J Theor Med 2003;5:183–218.
[35] Anand M, Rajagopal K, Rajagopal KR. A model for the formation and lysis of blood clots. Pathophysiol Haemost Thromb 2005;34:109–20.
[36] Bodnár T, Sequeira A. Numerical simulation of the coagulation dynamics of blood. Comput Math Methods Med 2008;9:83–104.
[37] Xu Z, Chen N, Kamocka MM, Rosen ED, Alber M. A multiscale model of thrombus development. J R Soc Interface 2008;5:705–22.
[38] Marée AM, Grieneisen V, Hogeweg P. The cellular Potts model and biophysical properties of cells, tissues and morphogenesis. In: Anderson AA, Chaplain MJ, Rejniak K, editors. Single-cell-based models in biology and medicine. Basel: Birkhäuser; 2007. p. 107–36.
[39] Xu Z, Lioi J, Mu J, Kamocka MM, Liu X, Chen DZ, et al. A multiscale model of venous thrombus formation with surface-mediated control of blood coagulation cascade. Biophys J 2010;98:1723–32.
[40] Xu Z, Chen N, Shadden SC, Marsden JE, Kamocka MM, Rosen ED, et al. Study of blood flow impact on growth of thrombi using a multiscale model. Soft Matter 2009;5:769–79.
[41] Oliver JA, Monroe DM, Roberts HR, Hoffman M. Thrombin activates factor XI on activated platelets in the absence of factor XII. Arterioscler Thromb Vasc Biol 1999;19:170–7.
[42] Wagenvoord R, Hemker PW, Hemker HC. The limits of simulation of the clotting system. J Thromb Haemost 2006;4:1331–8.
[43] van't Veer C, Mann KG. Regulation of tissue factor initiated thrombin generation by the stoichiometric inhibitors tissue factor pathway inhibitor, antithrombin-III, and heparin cofactor-II. J Biol Chem 1997;272:4367–77.
[44] Hemker HC, Béguin S. Thrombin generation in plasma: its assessment via the endogenous thrombin potential. Thromb Haemost 1995;74:134–8.
[45] Okorie UM, Denney WS, Chatterjee MS, Neeves KB, Diamond SL. Determination of surface tissue factor thresholds that trigger coagulation at venous and arterial shear rates: amplification of 100 fM circulating tissue factor requires flow. Blood 2008;111:3507–13.
[46] Shen F, Kastrup CJ, Liu Y, Ismagilov RF. Threshold response of initiation of blood coagulation by tissue factor in patterned microfluidic capillaries is controlled by shear rate. Arterioscler Thromb Vasc Biol 2008;28:2035–41.
[47] Sorensen EN, Burgreen GW, Wagner WR, Antaki JF. Computational simulation of platelet deposition and activation: I. model development and properties. Ann Biomed Eng 1999;27:436–48.
[48] Liu L, Freedman J, Hornstein A, Fenton JW, Ofosu FA. Thrombin binding to platelets and their activation in plasma. Br J Haematol 1994;88:592–600.
[49] Frojmovic MM, Mooney RF, Wong T. Dynamics of platelet glycoprotein IIb-IIIa receptor expression and fibrinogen binding. I. Quantal activation of platelet subpopulations varies with adenosine diphosphate concentration. Biophys J 1994;67:2060–8.
[50] Frojmovic MM, Mooney RF, Wong T. Dynamics of platelet glycoprotein IIb–IIIa receptor expression and fibrinogen binding. II. Quantal activation parallels platelet capture in stir-associated microaggregation. Biophys J 1994;67:2069–75.
[51] Gerotziafas GT, Depasse F, Busson J, Leflem L, Elalamy I, Samama MM. Towards a standardization of thrombin generation assessment: the influence of tissue factor, platelets and phospholipids concentration on the normal values of thrombogram–trombinoscope assay. Thrombosis J 2005:3.
[52] SBtoolbox. Systems Biology Toolbox for MATLAB: a computational platform for research in systems biology. Bioinform Biol Insights 2006;22:514–5.
[53] Hemker HC, Giesen P, Al Dieri R, Regnault V, ronique e, de Smedt E, et al. Calibrated automated thrombin generation measurement in clotting plasma. Pathophysiol Haemost Thromb 2003;33:4–15.
[54] Allen G, Wolberg A, Oliver J, Hoffman M, Roberts H, Monroe Dr. Impact of procoagulant concentration on rate, peak and total thrombin generation in a model system. J Thromb Haemost 2004;2:402–13.
[55] Ninivaggi M, Apitz-Castro R, Dargaud Y, de Laat B, Hemker HC, Lindhout T. Whole-blood thrombin generation monitored with a calibrated automated thrombogram-based assay. Clin Chem 2012;58:1252–9.
[56] Whelihan MF, Mann KG. The role of the red cell membrane in thrombin generation. Thromb Res 2013;131:377–82.
[57] Brummel-Ziedins K. Models for thrombin generation and risk of disease. J Thromb Haemost 2013;11:212–23.
[58] van Dijk K, van der Bom JG, Lenting PJ, de Groot PG, Mauser-Bunschoten EP, Roosendaal G, et al. Factor VIII half-life and clinical phenotype of severe hemophilia A. Haematologica 2005;90:494–8.
[59] Bonderman D, Teml A, Jakowitsch J, Adlbrecht C, Gyöngyösi M, Sperker W, et al. Coronary no-reflow is caused by shedding of active tissue factor from dissected atherosclerotic plaque. Blood 2002;99:2794–800.
[60] Arabinda Guha RB, Konigsberg W, Nemerson Y. Affinity purification of human tissue factor: interaction of factor VII and tissue factor in detergent micelles. Biochemistry (Mosc) 1986;83:299–302.
[61] Van Veen J, Gatt A, Makris M. Thrombin generation testing in routine clinical practice: are we there yet? Br J Haematol 2008;142:889–903.
[62] Hemker HC, Giesen P, Ramjee M, Wagenvoord R, Béguin S. The thrombogram: monitoring thrombin generation in platelet rich plasma. Thromb Haemost 2000;83:589–91.